Online Submissions: wjg.wjgnet.com
wjg@wjgnet.com
doi:10.3748/wjg.14.5557

World J Gastroenterol 2008 September 28; 14(36): 5557-5563
World Journal of Gastroenterology ISSN 1007-9327

Gene expression and MR diffusion-weighted imaging after chemoembolization in rabbit liver VX-2 tumor model

You-Hong Yuan, En-Hua Xiao, Jian-Bin Liu, Zhong He, Ke Jin, Cong Ma, Jun Xiang, Jian-Hua Xiao, Wei-Jian Chen

You-Hong Yuan, Jian-Bin Liu, Department of Radiology, Hunan Province People's Hospital, Changsha 410005, Hunan Province, China
En-Hua Xiao, Zhong He, Cong Ma, Jun Xiang, Department of Radiology, the Second Xiang-Ya Hospital, Central South University, Changsha 410005, Hunan Province, China
Ke Jin, Wei-Jian Chen, Department of Pathology, Hunan Province Children's Hospital, Changsha 410005, Hunan Province, China
Jian-Hua Xiao, Department of Epidemiology, Center for Disease Control of Hunan Province, Changsha 410005, Hunan Province, China
Author contributions: Yuan YH, Xiao EH designed research; Yuan YH, Xiao EH, Liu JB, He Z, Jin K, Ma C, Xiang J, Xiao JH, Chen WJ performed research; Yuan YH analyzed data; and Yuan YH, Xiao EH wrote the paper.
Supported by The National Natural Science Foundation of China, No. 30070235 and 30470508; The Natural Science Foundation of Hunan Province, No. 08JJ5043; The Science and Technology Foundation of Hunan Province, No. 06FJ3120 and 2007SK3072; and The Medical Science and Technology Foundation of Hunan Province, No. B2006-159
Correspondence to: Dr. You-Hong Yuan, Department of Radiology, Hunan Province People's Hospital, Changsha 410005, Hunan Province,
China. heyuanyouhong@yahoo.com.cn
Telephone: +86-731-2278047 Fax: +86-731-2278047
Received: Mary 3, 2008 Revised: August 26, 2008
Accepted: September 2, 2008
Published online: September 28, 2008

Abstract

AIM: To investigate the dynamic characteristics and the correlation between PCNA, Bax, nm23, E-cadherin expression and apparent diffusion coefficient (ADC) on MR diffusion-weighted imaging (DWI) after chemoembolization in rabbit liver VX-2 tumor model.

METHODS: Forty New Zealand rabbit liver VX-2 tumor models were included in the study. DWI was carried out periodically after chemoembolization. All VX-2 tumor samples in each group were examined by histopathology and Strept Avidin-Biotin Complex (SABC) immunohistochemical staining.

RESULTS: The PCNA expression index in VX-2 tumors was higher than in the normal parenchyma around the tumor ($P < 0.001$). Nm23, Bax or E-caderin expression index in VX-2 tumors were lower than in the normal parenchyma around the tumor (all $P < 0.001$). PCNA and nm23 expression in the VX-2 tumor periphery first increased and then decreased ($P < 0.001$ and $P = 0.03$, respectively), while the expression of Bax and E-cadherin before and after chemoembolization was insignificant. When b-value was 100 s/mm^2, there was a linear correlation between PCNA expression and ADC in the area of VX-2 tumor periphery ($P < 0.001$), and PCNA expression in VX-2 tumor periphery influenced the ADC.

CONCLUSION: The potential of VX-2 tumor infiltrating and metastasizing decreases, while its ability to proliferate increases for a short time after chemoembolization. To some degree, the ADC value indirectly reflects the proliferation of VX-2 tumor cells.

Key words: Rabbit liver; VX-2 tumor; Chemoembolization; Diffusion-weighted imaging; Gene expression

Peer reviewer: Dr. Serdar Karakose, Professor, Department of Radiology, Meram Medical Faculty, Selcuk University, Konya 42080, Turkey

Yuan YH , Xiao EH , Liu JB, He Z, Jin K, Ma C, Xiang J, Xiao JH, Chen WJ. Gene expression and MR diffusion-weighted imaging after chemoembolization in rabbit liver VX-2 tumor model. *World J Gastroenterol* 2008; 14(36): 5557-5563 Available from: URL: http://www.wjgnet.com/1007-9327/14/5557.asp DOI: http://dx.doi.org/10.3748/wjg.14.5557

INTRODUCTION

Hepatocellular carcinoma is one of the most common malignant tumors worldwide. The genetic mutation and abnormal gene expression of hepatocellular carcinoma during its origin, progression and after transcatheter arterial chemoembolization (TACE) have been investigated in several clinical and experimental studies, with respect to PCNA, Bax, E-caderin (E-cad) and nm23 gene expression

The expression of Proliferating Cell Nuclear Antigen (PCNA) is high in the S, G_2 and M stages of cell division, and low in the G_0 and G_1 stages. The degree of PCNA expression reflects cellular reproductive activity, which correlates significantly and positively with

the pathological grade, the potential for recurrence, and survival time of malignant tumors. Therefore, it is important to measure the degree of PCNA expression in evaluating the malignant potential and prognosis of tumors[1-5]. Shi *et al*[4] observed that the degree of PCNA expression correlated with the size, invasive potential and degree of enhancement on CT scan of hepatocellular carcinoma. As a member of the Bcl-2 family, Bax gene is an important apoptotic controlling gene. Most investigations have demonstrated that Bax is a protein-inducing apoptosis, which promotes cell apoptosis and suppresses cell proliferation through multiple mechanism[6-9]. The nm23-H1 gene expresses nucleoside diphosphate kinase (ndpk), and has a significant impact on tumor metastasis. As reported in several studies, low expression of nm23 and the absence of alleles correlates with a high rate of infiltration and metastasis in many tumors, including hepatocellular carcinoma[4-10]. The coding product of E-cad gene is a transmembrane glycoprotein that is calcium depended and is able to mediate adhesion between cells. When it is low or absent, the adhesion between cells decreases, enabling the cancer cells to separate easily from the primary tumor, resulting in local infiltration and distant metastasis[10].

Diffusion-weighted imaging (DWI) is used much less frequently in the diagnosis of hepatic tumor and for the evaluation of tumor progression, because of its poor imaging quality[11-14]. With the development of MRI software and scanning technology, especially for echoplanar imaging (EPI) in recent years, many deficiencies, such as poor imaging quality and slow scanning speed, have been resolved[15-17]. As reported by several workers (Ichikawa *et al*[18,19], Yamashita *et al*[20], Taouli *et al*[21], Sun *et al*[22] and Yang *et al*[23,24]), the apparent diffusion coefficient (ADC) of hepatic cysts, hemangioma, hepatocellular carcinoma, metastatic lesions, normal parenchyma and liver cirrhosis decrease gradually on DWI. The ADC of hepatic cysts is the highest, while ADC of benign tumors is higher than that of malignant tumors. Colagrande *et al*[25] demonstrated that coagulation necrosis had low signal compared to viable tumor. Kamel *et al*[26] confirmed these findings in a study on 8 patients with hepatocellular carcinoma; ADC increased with the degree of tumor necrosis, and in 6 tumors the DWI values were higher compared to the normal parenchyma. Based on these observations, DWI, and especially ADC have potential value of differentiating benign tumor from malignant tumor.

However, few studies have been carried out to investigate the dynamic characteristics of hepatocellular carcinoma gene expression after chemoembolization. Moreover, the ADC of hepatocellular carcinoma on DWI has not been investigated by image-pathology-gene expression.

The purpose of the present study was to investigate the dynamic characteristics of PCNA, Bax, nm23 and E-cad expression after chemoembolization, and to evaluate the correlation between ADC on DWI and gene expression in rabbit VX-2 tumor model. However, the signal dynamic characteristics on DWI and the pathological mechanisms will be discussed in separate report.

MATERIALS AND METHODS

Animals and establishment of VX-2 tumor model

Animal studies were carried out under the supervision of a veterinarian according to the guidelines on the Use of Laboratory Animals of the Ministry of Public Health of China. All animals were provided by the Laboratory Animal Center of the Second Xiangya Hospital and all protocols were approved by the Animal Use and Care Committee of the Second Xiangya Hospital.

Forty New Zealand rabbits were included in the study. Twenty-two were male and eighteen were female rabbits. The weight ranged from 1.7 kg to 2.5 kg, and the ages from 5 mo to 6 mo. All New Zealand white rabbits were healthy. Forty-seven rabbit VX-2 tumor models were developed by implanting directly into the liver, after opening the abdominal cavity. The rabbit VX-2 tumor strain was provided by the Fourth Military Medical University.

Forty VX-2 tumor models were chosen randomly from forty-seven VX-2 tumor models and were divided into four groups, a control group (non-interventional group, group A) and three investigation groups (group A, 16 h after chemoembolization; group B, 32 h after chemoembolization; and group C, 48 h after chemoembolization).

Interventional protocol

After DWI was performed on the 21st day after implantation, trans-hepatic artery catheterization chemoembolization was carried out in the animal operating room of the Second Xiangya Hospital, in study groups B, C and D.

First, the rabbits were anesthetized by injecting 3% soluble pentobarbitone. The abdominal skin was then disinfected, and the abdomen was opened by incising through the skin and the musculi recti abdominis. The organs of hepatic hilar region were exposed and the different structures such as arteria coeliaca, arteria hepatica communis, arteria hepatica propria, arteria gastroduodenalis and portal vein were recognized. The distal end of arteria gastroduodenalis was occluded, and a drop of aethocaine was placed on it. The arteria gastroduodenalis was punctured and a plastic transfixion pin was introduced and advanced into arteria hepatica propria, followed by infusion of iodized oil (0.3 mL/kg) and pharmorubicin (2 mg/kg). Finally, after making certain that there was no bleeding from the liver and other structures, the abdominal membrane, musculature and skin were sutured layer by layer.

Magnetic resonance imaging protocol

After the animals were anesthetized with 3% soluble pentobarbitone at a dose of 1 mL/kg or with different

Table 1 Gene expression of different areas of VX-2 tumour and the normal parenchyma around the tumor (%)

	PCNA	nm23	Bax	E-cad
Normal parenchyma	8.28 ± 5.61	16.53 ± 14.66	40.00 ± 23.72	78.15 ± 18.35
Tumor outer layer	65.45 ± 3.43	1.74 ± 4.07	1.91 ± 2.66	6.18 ± 7.55
Tumor periphery area	72.73 ± 14.23	0.42 ± 0.64	1.05 ± 1.09	1.96 ± 1.79
Tumor center area	58.37 ± 15.25	6.74 ± 10.13	2.16 ± 4.59	1.55 ± 3.65

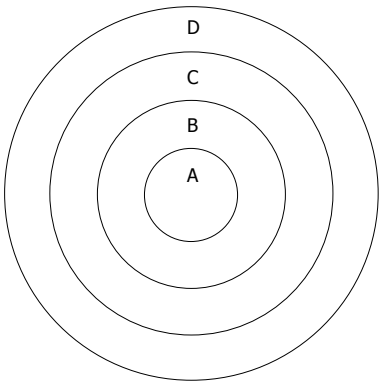

Figure 1 A-D represent VX-2 tumor center, VX-2 tumor periphery, VX-2 tumor outer layer and normal liver parenchyma around tumor respectively. The ADC levels and signal were measured on DWI, and the samples were investigated by histopathology.

doses based on the animal status, in order to make certain that the animals had stable breathing, DWI(axial) was performed on a 1.5-Tesla Signa Twinspeed MR scanner (General Electron Medical Systems, USA), using a small diameter cylindrical brain radiofrequency coil. The scans were done before chemoembolization, and again at 6 h, 16 h, 32 h and 48 h after chemoembolization. The DWI scanning parameters included spin echo echoplanar imaging (SE-EPI) series, *b*-value 100 and 300 s/mm^2, repetition time (TR) 6000 ms, echo time (TE) 45 ms, 20 cm × 15 cm field of view (FOV), 8 NEX, 2 mm thickness layer, and 0.5 mm Space, 128 × 128 matrix.

The ADC values and signal values were obtained in the VX-2 tumor periphery, VX-2 tumor center and normal liver parenchyma around the tumor (Figure 1) using Function software in GE workstation. Three different regions of interest (ROIs, 50 mm^2 each area) were chosen in the normal liver parenchyma (area D in Figure 1). The average reading was considered as the ADC value or the signal value of the normal liver parenchyma around the tumor. The thickness of the area A and B in Figure 1 was respectively two fifth of the diameter of the VX-2 tumor. Similarly, the average readings of three different ROIs ADC values or signal values in area B were considered as the ADC value or the signal value of VX-2 tumor periphery. The ADC value or signal value of area A was the center of the VX-2 tumor. All measurements were made by two senior attending physicians or associate professors.

Immunohistochemical staining protocol

DWI was performed before chemoembolization, and 16 h, 32 h and 48 h after chemoembolization. The rabbits were then sacrificed by injecting an overdose of 3% soluble pentobarbitone. Under aseptic conditions, we obtained layer by layer VX-2 samples (Figure 1). Each VX-2 tumor was divided into the outer layer area, the periphery area and center area (Figure 1). All tissue samples were fixed in formaldehyde for 24 h before embedding in mineral wax.

Immunohistochemical staining was performed, using the SP method. Monoclonal antibody against PCNA, Bax, nucleoside diphosphate kinase (ndpk, expression product of nm23 gene) and e-cadherin endogenous avidin and biotin block ade solution, biotin-marked SP were used for immunostaining. PBS was used as a negative control, and all the results were negative. A known positive specimen of mammary adenocarcinoma was used as a positive control for PCNA, Bax and ndpk instead of PHC tissue, while pancreatic carcinoma was used for E-cad; the results were all positive.

Expression index was used to estimate the degree of gene expression, which was based on the contrast of positive cells with the total number of cells, as seen under the microscope. When the cell nucleus appeared as brown-yellow with PCNA immunohistochemical staining, the PCNA expression was considered as positive. When cytolymph appeared as brown-yellow in Bax, nm23 or E-cad immunohistochemical staining, the test was considered as positive. Ten random locations were examined under a 400 × microscope in non-necrotic areas, and the number of PCNA, Bax, nm23 and E-cad expressing cells as well as the total number of cells were counted in a double blind fashion by two investigators who were not part of our study group. The average value was considered as the expression index. When the antibody was replaced by the balanced solution, all the gene expressions were negative.

Statistical analysis

Based on the apparent diffusion coefficient (ADC) value of ROIs and expression index of PCNA, Bax, nm23 and E-cad, the differences between the different areas, the different time groups and the correlation between ADC and gene expression was assessed. The statistical significance was calculated by analysis of variance (ANOVA), non-parameter and multiple linear regression, using the SPSS 12.0 software.

RESULTS

Gene expression information of VX-2 tumor

The results of PCNA, nm23, Bax and E-cad expression in VX-2 tumors and in the normal parenchyma around the tumor before chemoembolization are shown in Table 1 and Figure 2.

The differences in the PCNA, Bax, nm23 and

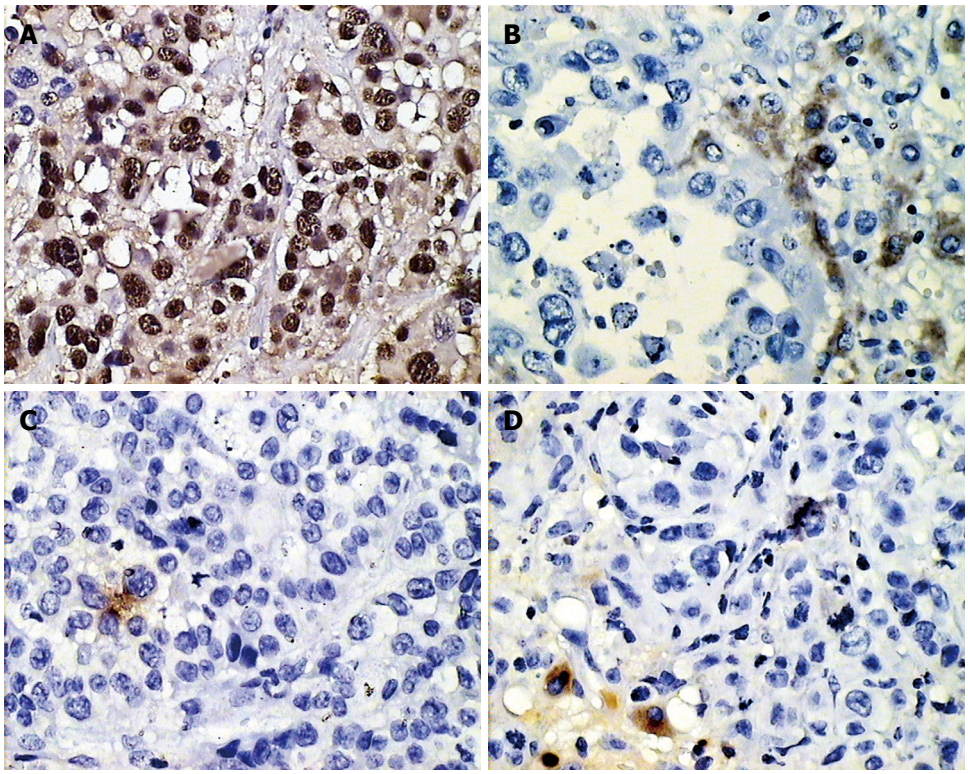

Figure 2 Positive gene expression in VX-2 tumor. **A**: PCNA; **B**: Bax; **C**: nm23; **D**: E-cad.

Table 2 Dynamic information of the gene expression in the peripheral area of VX-2 tumor and the normal parenchyma around the tumor (%)

Time	Area	PCNA	nm23	Bax	E-cad
A time	E	72.73 ± 14.23	0.42 ± 0.64	1.05 ± 1.09	1.96 ± 1.79
	F	8.28 ± 5.61	16.53 ± 14.66	40.00 ± 23.72	78.15 ± 18.35
B time	E	80.04 ± 22.84	2.29 ± 1.58	0.86 ± 1.44	2.87 ± 2.04
	F	4.04 ± 2.06	57.35 ± 28.36	81.22 ± 23.31	86.41 ± 12.65
C time	E	92.60 ± 4.76	7.56 ± 8.88	0.45 ± 0.57	0.93 ± 1.48
	F	21.87 ± 24.59	67.64 ± 30.54	85.63 ± 20.51	91.03 ± 9.65
D time	E	87.63 ± 7.12	4.14 ± 4.71	0.78 ± 1.05	1.07 ± 0.81
	F	19.38 ± 17.74	40.84 ± 34.90	87.08 ± 10.16	91.03 ± 5.11

A time is before chemoembolization or on 21th day after implantation. B time, C time, and D time represent samples obtained after 16 h, 32 h and 48 h after chemoembolization respectively. E indicates the peripheral area of VX-2 tumor and F normal parenchyma around VX-2 tumor.

E-cad expression index in the different areas before chemoembolization were statistically significant (χ^2 = 19.08, $P < 0.001$; χ^2 = 20.165, $P < 0.001$; χ^2 = 12.86, $P < 0.001$; χ^2 = 22.20, $P < 0.001$). The differences in the PCNA, Bax, nm23 and E-cad expression index between the tumor periphery and the normal parenchyma around the tumor were statistically significant (Z = -5.51, $P < 0.001$; Z = -5.39, $P < 0.001$; Z = -5.51, P = 0.003; Z = -5.511, $P < 0.001$).

The results of PCNA, nm23, Bax and E-cad expression in groups A, B, C, and D in the VX-2 tumor periphery and normal parenchyma around the tumor are shown in Table 2 and Figure 2.

The differences in the PCNA, nm23 and Bax expression in the normal parenchyma between groups A, B, C, and D were statistically significant (χ^2 = 10.92, P = 0.04; χ^2 = 14.83, $P < 0.001$; χ^2 = 17.28, P = 0.03), but E-cad expression was not significant (χ^2 = 3.410, $P > 0.05$). The differences in PCNA and nm23 expression in the tumor periphery between groups A, B, C, and D were significant (χ^2 = 14.37, $P < 0.001$; χ^2 = 8.94, P = 0.03) but that for Bax and E-cad were not significant (χ^2 = 1.98, $P > 0.05$; χ^2 = 3.88, $P > 0.05$).

Table 3 ADC values of the tumor and normal parenchyma (mean ± SD, × 10^{-3} mm^2/s)

	ADC in tumor periphery area		ADC in normal parenchyma	
	b = 100	b = 300	b = 100	b = 300
A time	1.71 ± 0.27	1.48 ± 0.23	2.71 ± 0.42	2.30 ± 0.40
B time	1.24 ± 0.22	1.12 ± 0.20	2.10 ± 0.54	1.65 ± 0.37
C time	1.48 ± 0.37	1.23 ± 0.16	2.10 ± 0.49	1.97 ± 0.29
D time	1.57 ± 0.23	1.40 ± 0.18	2.43 ± 0.33	2.06 ± 0.23

A time is before chemoembolization or on the 21th day after implantation. B time, C time, and D time represent samples obtained after 16 h, 32 h and 48 h after chemoembolization respectively.

Dynamic ADC values before and after chemoembolization (Table 3, Figures 3 and 4)

When the b-value was 100 s/mm^2, there was a significant correlation between the expression index of PCNA, nm23, Bax, E-cad and ADC values in the normal parenchyma around VX-2 tumor (r = -0.50, $P < 0.001$; r = -0.38, P = 0.08; r = -0.27, P = 0.04; r = -0.25; P = 0.04) . There was a linear correlation between PCNA and nm23 expression index and ADC value (F = 8.15, $P < 0.001$), and PCNA and nm23 expression influenced ADC. There was a linear correlation between PCNA expression index and ADC value in the VX-2 tumor periphery (F = 32.69, $P < 0.001$), while PCNA

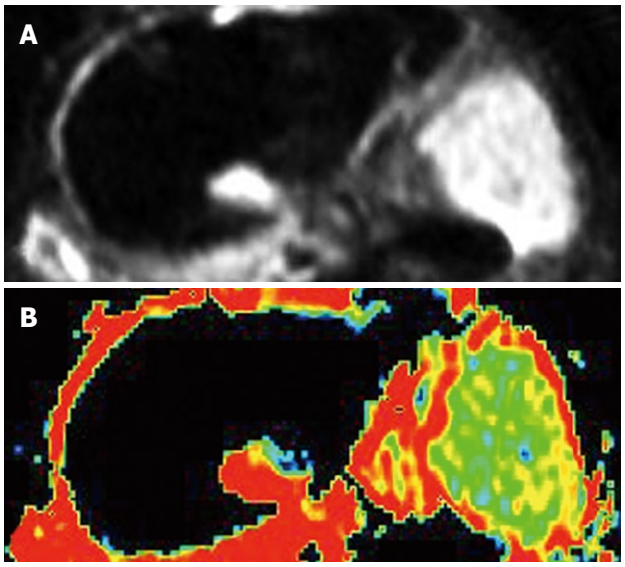

Figure 3 Image manifestations of hepatic VX-2 tumor on DWI and ADC map when b-value was 100 s/mm^2, 6 h after chemoembolization. **A**: High signal and distinct margins of VX-2 tumor on DWI; **B**: Low signal on the ADC map.

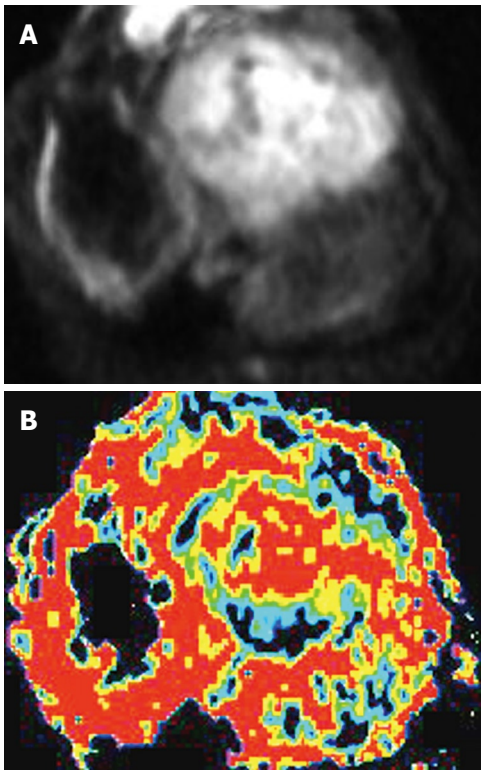

Figure 4 High uneven signal and distinct margins of hepatic VX-2 tumor on DWI and ADC map when b-value was 100 s/mm^2, 32 h after chemoembolization. **A**: High and uneven signal and distinct margins on DWI; **B**: Low or equal signal on ADC map.

expression influenced ADC. However, there was no correlation between nm23, Bax and E-cad expression index, and ADC value (r = -0.20, P = 0.11; r = 0.17, P = 0.15; r = -0.10, P = 0.28).

When the b-value was 300 s/mm^2, there was a correlation between PCNA, nm23, Bax and E-cad expression index, and ADC value in the normal parenchyma around VX-2 tumor (r = -0.37, P = 0.01; r = -0.37, P = 0.01; r = -0.28, P = 0.04; r = -0.31, P = 0.03), and there was a linear correlation between PCNA and nm23 expression index and ADC value (F = 5.00, P < 0.05), and PCNA and nm23 expression influenced ADC. There was a linear correlation between PCNA expression index and ADC value in the VX-2 tumor periphery (F = 29.08, P < 0.001), and PCNA expression influenced ADC, but there was no correlation between nm23, Bax and E-cad expression index and ADC value in the VX-2 tumor periphery (r = -0.15, P = 0.18; r = 0.14, P = 0.19; r = -0.04, P = 0.40).

DISCUSSION

Before and after chemoembolization, PCNA expression was significantly higher in VX-2 tumors compared with the normal parenchyma, whereas nm23, Bax and E-cad expression in the normal parenchyma was significantly higher. PCNA expression in the VX-2 tumor periphery was higher compared to the tumor outer layer and its center, while nm23 and Bax expression in the VX-2 tumor center were higher compared to the outer layer and the peripheral area of the tumor. The high level of PCNA expression indicated that the VX-2 tumor cells had powerful heteromorphism and reproductive activity. The considerable reduction in Bax expression resulted in a decrease in cell apoptosis such that the cell reproductive activity increased, while the reduction in nm23 and E-cad expression led to a marked increase in the ability of the tumor to infiltrate and metastasize. In general, the VX-2 tumor had a high malignant potential, with capacity for rapid reproduction, infiltration and metastasis.

At the same time, the ADC values of VX-2 tumor were significantly lower than the normal parenchyma, and ADC showed an inverse correlation with PCNA expression, but not with nm23, Bax and E-cad expression. These findings suggest that the ability of cell proliferation increases because gene expression increases relative to tumor proliferation such that water molecular diffusion is limited and ADC decreases. In other words, reduction in ADC indirectly increases the gene expression relative to the tumor proliferation. Similarly, Ding *et al*[27] reported that decrease in E-cad expression leads an increase in tumor reproductive activity and Luo *et al*[5] demonstrated that nm23 expression had an inverse correlation with PCNA. To a certain extent, tumor ADC can reflect its ability to infiltrate and metastasize.

After chemoembolization, PCNA expression in VX-2 tumors was slightly higher than before chemoembolization. PCNA expression increased gradually until 32 h, and then decreased slightly. PCNA expression in the normal parenchyma was significantly lower than that in VX-2 tumors, and its expression increased after chemoembolization. Soon after chemoembolization, the tumor reproductive activity may increase, but then decreases which may be related to the stimulation caused by chemoembolization. Therefore, the frequency of chemoembolization should be determined

carefully because viable tumor cells may have powerful reproductive activity. In the present study, the increase in the reproductive activity of normal parenchyma cells may be related to nonselective catheterization, indicating the importance of selective catheterization. After chemoembolization, nm23 expression in the VX-2 tumor or normal parenchyma was higher than before chemoembolization, and it continued to increase until 32 h, followed by decreased expression. These findings indicate that the risk of tumor metastasis may decrease after chemoembolization. The expression of E-cad and Bax in the tumors did not show a significant change after chemoembolization, while E-cad and Bax expression increased in the normal parenchyma. On the other hand, both with b-value 100 s/mm^2 and b-value 300 s/mm^2, the ADC levels in the VX-2 tumor periphery decreased gradually until 16 h after chemoembolization, and then increased gradually. The ADC level in the tumor was inversely related to PCNA expression. Besides water molecules "Brownian Motion", to a certain degree the ADC value indirectly impacts the reproductive activity of cells. With an increase in tumor cell reproduction, the diffusion motion of water cells becomes limited, such that the ADC value decreases. This may be one of the reasons why the ADC of malignant tumors is lower than that of benign tumors. Therefore, the ADC value has potential in the diagnosis and differentiation of tumors, as reported in previous studies by Ichikawa *et al*[18,19], Yamashita *et al*[20] and Kim *et al*[28].

ACKNOWLEDGMENTS

We thank the staff of the Radiology Department and the Laboratory Animal Center of the Second Xiangya Hospital for their help and support, especially Miss Ying-Si He.

COMMENTS

Background

Diffusion-weighted imaging (DWI) has not been extensively used in the diagnosis as well as in the evaluation of the progression and outcome of hepatic tumors, and few studies have been carried out to investigate the dynamic characteristics of hepatocellular carcinoma gene expression after chemoembolization. We believe that DWI has the potential value of differentiating benign tumors from malignant tumors after chemoembolization. In the present study, we investigated the characteristics of proliferating cell nuclear antigen (PCNA), Bax, nm23 and E-cadherin (E-cad) expression after chemoembolization, and evaluated the correlation between the apparent diffusion coefficient (ADC) on DWI and gene expression, in the rabbit VX-2 tumor model.

Research frontiers

There are very few studies on hepatic pathological changes on DWI. The ADC value of benign lesions, such as hepatic cysts and hemangiomas was higher than that of malignant lesions such as hepatocellular carcinoma and metastasis. Several studies have shown that signals from areas of tumor coagulation necrosis are lower compared to tumor viable areas. Several studies have reported on the PCNA, Bax, nm23 and E-cad expression after chemoembolization. However, few studies have investigated the dynamic characteristics of hepatocellular carcinoma gene expression after chemoembolization, using image-pathology-gene expression

Innovations and breakthroughs

The present study clearly demonstrates that DWI has the potential application of detecting and differentiating viable tumors from necrotic tumors after chemoembolization. PCNA expression in VX-2 tumors was slightly higher compared to the level before chemoembolization. The nm23 expression in VX-2 tumor was higher, such that the potential for VX-2 tumor to infiltrate and metastasize decreases, while the ability to proliferate increases for a short period after chemoembolization. To some extent, the ADC value is able to indirectly reflect the proliferation of VX-2 tumor cells.

Applications

Physicians can apply this knowledge to evaluate hepatic tumors that are clearly progressive in nature, and accurately differentiate areas of necrotic tumor from viable tumor after chemoembolization, as well as determine to some extent the proliferation of VX-2 tumor cells on ADC.

Peer review

This is an interesting, well designed and written study on the clinical significance of diffusion-weighted imaging. The manuscript contains important information on the manifestations of viable, necrotic and liquefied or cystic areas in liver tumors.

REFERENCES

1 **Nan KJ**, Ruan ZP, Jing Z, Qin HX, Wang HY, Guo H, Xu R. Expression of fragile histidine triad in primary hepatocellular carcinoma and its relation with cell proliferation and apoptosis. *World J Gastroenterol* 2005; **11**: 228-231

2 **Nan KJ**, Jing Z, Gong L. Expression and altered subcellular localization of the cyclin-dependent kinase inhibitor p27Kip1 in hepatocellular carcinoma. *World J Gastroenterol* 2004; **10**: 1425-1430

3 **Nanashima A**, Yano H, Yamaguchi H, Tanaka K, Shibasaki S, Sumida Y, Sawai T, Shindou H, Nakagoe T. Immunohistochemical analysis of tumor biological factors in hepatocellular carcinoma: relationship to clinicopathological factors and prognosis after hepatic resection. *J Gastroenterol* 2004; **39**: 148-154

4 **Shi YH**, Wang B, Zhu YL, Gao ZQ. Correlation of Spiral CT Signs with the Expression of p21~(WAF1), p16~(INK4) and PCNA in HCC. *Linchuang Fangshexue Zazhi* 2003; **22**: 847-851

5 **Luo HY**, Wang HC, Feng DY. [Expression of proliferating cell nucleus antigen and nm23 protein and their relation with metastasis in hepatocellular carcinoma] *Hunan Yikedaxue Xuebao* 2003; **28**: 17-19

6 **Simile MM**, Pagnan G, Pastorino F, Brignole C, De Miglio MR, Muroni MR, Asara G, Frau M, Seddaiu MA, Calvisi DF, Feo F, Ponzoni M, Pascale RM. Chemopreventive N-(4-hydroxyphenyl)retinamide (fenretinide) targets deregulated NF-{kappa}B and Mat1A genes in the early stages of rat liver carcinogenesis. *Carcinogenesis* 2005; **26**: 417-427

7 **Osada S**, Saji S, Kuno T. Clinical significance of combination study of apoptotic factors and proliferating cell nuclear antigen in estimating the prognosis of hepatocellular carcinoma. *J Surg Oncol* 2004; **85**: 48-54

8 **Xiao EH**, Liu DT, Shen SB, Zhou SK, Tan LH, Wang YH, Luo JG, Wu YZ, Tan CL, Liu H, Zhu H. Effect of preoperative transcatheter arterial chemoembolization on apoptosis of hepatocellular carcinoma cells. *Zhonghua Yixue Zazhi* 2003; **116**: 203-207

9 **Xiao EH**, Hu GD, Li JQ. Relationship between apoptosis and invasive and metastatic potential of hepatocellular carcinoma. *Hepatobiliary Pancreat Dis Int* 2002; **1**: 574-576

10 **Miyoshi A**, Kitajima Y, Sumi K, Sato K, Hagiwara A, Koga Y, Miyazaki K. Snail and SIP1 increase cancer invasion by upregulating MMP family in hepatocellular carcinoma cells. *Br J Cancer* 2004; **90**: 1265-1273

11 **Chan JH**, Tsui EY, Luk SH, Fung AS, Yuen MK, Szeto ML, Cheung YK, Wong KP. Diffusion-weighted MR imaging of the liver: distinguishing hepatic abscess from cystic or necrotic tumor. *Abdom Imaging* 2001; **26**: 161-165

12 **Moteki T**, Horikoshi H, Oya N, Aoki J, Endo K. Evaluation of hepatic lesions and hepatic parenchyma using diffusion-weighted reordered turboFLASH magnetic resonance

images. *J Magn Reson Imaging* 2002; **15**: 564-572
13 **Aube C**, Racineux PX, Lebigot J, Oberti F, Croquet V, Argaud C, Cales P, Caron C. [Diagnosis and quantification of hepatic fibrosis with diffusion weighted MR imaging: preliminary results] *J Radiol* 2004; **85**: 301-306
14 **Chow LC**, Bammer R, Moseley ME, Sommer FG. Single breath-hold diffusion-weighted imaging of the abdomen. *J Magn Reson Imaging* 2003; **18**: 377-382
15 **Boulanger Y**, Amara M, Lepanto L, Beaudoin G, Nguyen BN, Allaire G, Poliquin M, Nicolet V. Diffusion-weighted MR imaging of the liver of hepatitis C patients. *NMR Biomed* 2003; **16**: 132-136
16 **Hori M**, Ichikawa T, Sou H, Tsukamoto T, Kitamura T, Okubo T, Araki T, Amemiya Y, Okamoto E, Obara M. [Improving diffusion-weighted imaging of liver with SENSE technique: a preliminary study] *Nippon Igaku Hoshasen Gakkai Zasshi* 2003; **63**: 177-179
17 **Murtz P**, Flacke S, Traber F, van den Brink JS, Gieseke J, Schild HH. Abdomen: diffusion-weighted MR imaging with pulse-triggered single-shot sequences. *Radiology* 2002; **224**: 258-264
18 **Ichikawa T**, Haradome H, Hachiya J, Nitatori T, Araki T. Diffusion-weighted MR imaging with a single-shot echoplanar sequence: detection and characterization of focal hepatic lesions. *AJR Am J Roentgenol* 1998; **170**: 397-402
19 **Ichikawa T**, Haradome H, Hachiya J, Nitatori T, Araki T. Diffusion-weighted MR imaging with single-shot echo-planar imaging in the upper abdomen: preliminary clinical experience in 61 patients. *Abdom Imaging* 1999; **24**: 456-461
20 **Yamashita Y**, Tang Y, Takahashi M. Ultrafast MR imaging of the abdomen: echo planar imaging and diffusion-weighted imaging. *J Magn Reson Imaging* 1998; **8**: 367-374
21 **Taouli B**, Martin AJ, Qayyum A, Merriman RB, Vigneron D, Yeh BM, Coakley FV. Parallel imaging and diffusion tensor imaging for diffusion-weighted MRI of the liver: preliminary experience in healthy volunteers. *AJR Am J Roentgenol* 2004; **183**: 677-680
22 **Sun XJ**, Quan XY, Liang W, Wen ZB, Zeng S, Huang FH, Tang M. [Quantitative study of diffusion weighted imaging on magnetic resonance imaging in focal hepatic lesions less than 3 cm] *Zhonghua Zhongliu Zazhi* 2004; **26**: 165-167
23 **Yang ZH**, Xie JX, Hu BF, Zhang YW, Zhou C. Evaluation of Liver Cirrhosis with Diffusion-weighted MR Imaging: An Experimental Study. *Zhongguo Yixue Yingxiang Jishu* 2002; **18**: 849-851
24 **Yang ZH**, Xie JX. Clinical application of diffusion weighted MR imaging in the liver. *Zhonghua Fangshexue Zazhi* 1999; **10**: 684-688
25 **Colagrande S**, Politi LS, Messerini L, Mascalchi M, Villari N. Solitary necrotic nodule of the liver: imaging and correlation with pathologic features. *Abdom Imaging* 2003; **28**: 41-44
26 **Kamel IR**, Bluemke DA, Ramsey D, Abusedera M, Torbenson M, Eng J, Szarf G, Geschwind JF. Role of diffusion-weighted imaging in estimating tumor necrosis after chemoembolization of hepatocellular carcinoma. *AJR Am J Roentgenol* 2003; **181**: 708-710
27 **Ding YL**, Zhao RY, You CZ, Li ZT. Study of the relation ship between expression of E cadherin and PCNA in hepatocellular carcinoma. *Zhonghua Zhongliu Fangzhi Zazhi* 2002; **9**: 556-557
28 **Kim T**, Murakami T, Takahashi S, Hori M, Tsuda K, Nakamura H. Diffusion-weighted single-shot echoplanar MR imaging for liver disease. *AJR Am J Roentgenol* 1999; **173**: 393-398

S- Editor Zhong XY **L- Editor** Anand BS **E- Editor** Lin YP